POWER AND CAPACITY FADE MECHANISM OF $LiNi_{0.8}Co_{0.15}Al_{0.05}O_2$ COMPOSITE CATHODES IN HIGH-POWER LITHIUM-ION BATTERIES

Robert Kostecki and Frank McLarnon

Environmental Energy Technologies Division
Lawrence Berkeley National Laboratory
University of California, Berkeley, CA 94720, USA

ABSTRACT

High-power Li-ion cells that were tested at elevated temperatures showed a significant impedance rise, which was associated primarily with the $LiNi_{0.8}Co_{0.15}Al_{0.05}O_2$ cathode. By systematically collecting thousands of Raman spectra from 50 x 80 μm areas at 0.9 μm spatial resolution, and integrating the respective bands of the cathode components for each spectrum, we were able to produce color-coded, semi-quantitative composition maps of cathode surfaces. Raman microscopy images of cathodes from tested cells revealed that cell cycling or storage at elevated temperatures led to significant changes in the $LiNi_{0.8}Co_{0.15}Al_{0.05}O_2$/elemental-carbon surface concentration ratio. The loss of conductive carbon correlated with the power and capacity fade of the tested cathodes. The cathode surface state of charge (SOC) varied between individual grains of active material, and at some locations the spectra indicated the presence of fully charged material, despite the deep cell discharge at the end of testing.

INTRODUCTION

The U.S. Department of Energy's Advanced Technology Development (ATD) Program supports the development of high-power Li-ion batteries for hybrid electric vehicle applications [1]. Included in the ATD Program are diagnostic evaluations of Li-ion cells that were aged and/or cycled under various conditions [2,3]. A primary goal of these diagnostic tests is to determine the mechanisms responsible for cell power loss that accompanies life tests at elevated temperatures. Li-ion cells that were stored or cycled at elevated temperatures showed a significant impedance rise and power loss during ageing and/or cycling. Impedance measurements of the cell components indicated that the $LiNi_{0.8}Co_{0.15}Al_{0.05}O_2$ cathode is primarily responsible for the observed cell power loss at elevated temperatures, similar to the $LiNi_{0.8}Co_{0.2}O_2$ cathode that was studied in our previous work [3]. Possible causes of the increase in cathode impedance include the formation of an electronic and/or ionic barrier at the cathode surface [4]. However, the observation that, in these cells, power fade is always accompanied by the loss of discharge capacity suggests that the mechanism of degradation is more complicated, may consist of multiple processes, and may be a somewhat general phenomenon that affects several types of cathodes.

X-ray diffraction spectroscopy failed to detect noticeable changes in the bulk structure of the tested cathodes, and no evidence of material structural degradation or

formation of new phases was found. In this study we focus on post-test analysis of $LiNi_{0.8}Co_{0.15}Al_{0.05}O_2$ cathodes removed from high-power Li-ion cells, which were stored and/or cycled at elevated temperatures. We focused our attention on cathode surface processes, which we believe have a dominant effect on impedance behavior. In the present report we demonstrate that current-sensing AFM and Raman microscopy can provide unique information on complex surface phenomena, which are likely responsible for the composite cathode capacity fade and impedance increase.

EXPERIMENTAL

High-power Li-ion cells with a $LiNi_{0.8}Co_{0.15}Al_{0.05}O_2$ cathode, a synthetic graphite anode, 1.2 M $LiPF_6$ + ethylene carbonate + ethyl-methyl carbonate (EC/EMC) electrolyte, and a Celgard® 2300 separator, were manufactured, aged, cycled, and/or abused and then characterized under the ATD Program [1]. We compared a fresh cathode with cathodes taken from cells that were aged or cycled at elevated temperatures for up to 68 weeks, losing up to 52% of their initial power and 24% of their initial capacity.

The samples were collected from the cathodes ~ 2.5 cm away from the current collector tab, washed in pure dimethyl carbonate (DMC), soaked in DMC for 30 minutes after removal from Li-ion cells, and stored in hermetic containers inside an argon-filled glove box. This procedure removed electrolyte salt from the electrode to prevent its reaction with air and moisture. An integrated Raman microscope system "Labram" made by ISA Groupe Horiba was used to analyze and map the cathode surface structure and composition. The excitation source was an internal He-Ne (632 nm) 10 mW laser. The power of the laser beam was adjusted to 0.1 mW with neutral filters of various optical densities. The size of the laser beam at the sample was ~1.2 μm.

We used current-sensing atomic force microscopy (CSAFM) to test and image the electronic conductivity of the $LiNi_{0.8}Co_{0.15}Al_{0.05}O_2$ powder (Fuji Chemical) and surface electronic conductivity of the composite cathodes from tested cells. The powder was pressed into a gold foil to produce randomly scattered particles of $LiNi_{0.8}Co_{0.15}Al_{0.05}O_2$ in good electronic contact with the Au substrate. *Ex-situ* CSAFM images were obtained with a Molecular Imaging (MI) scanning probe microscope coupled with a Park Scientific Instruments (PSI) electronic controller. The Si atomic force microscope (AFM) tips were coated with a thin conductive layer of W_2C. All CSAFM experiments were performed in constant-force mode with controlled oxide-tip voltage difference. A single scan of the tip over the specimen simultaneously produced two images: a topographic image and a conductance image; the latter represents oxide-tip current variations during scanning at a given oxide-tip voltage difference. CSAFM imaging was conducted in a small glove box specially designed for scanning-probe microscopy tests under a controlled N_2 atmosphere.

RESULTS AND DISCUSSION

Figure 1 shows CSAFM images of a representative 5 x 5 μm area of the $LiNi_{0.8}Co_{0.15}Al_{0.05}O_2$ cathodes from a fresh cell and a cell stored at 55°C, 60% SOC, which lost 34% of its power and 16% of its capacity. Examination of the topographic AFM images of the fresh and tested cathodes shows no significant change in the surface

morphology. That observation is in contrast to our previous results of the $LiNi_{0.8}Co_{0.2}O_2$ composite electrodes, which exhibited considerable amounts of nanocrystalline deposit in the inter-granular spaces and across the crystal planes of the active material in the cells tested at elevated temperatures [2].

The right-hand panel of Fig. 1 is the oxide-tip current response (conductance image) of the same area as shown the left-hand panel at a 1.0 V voltage difference, *i.e.*, the cathode sample was poised at a positive potential *vs*. the CSAFM tip. In the conductance image, a dark color represents high electronic conductance, whereas a white color corresponds to areas of low or zero electronic conductance. Taking into account that the tip is in physical contact with the oxide, the magnitude of the current is determined by the local electronic properties of the electrode and the tip, and the tip-sample voltage difference.

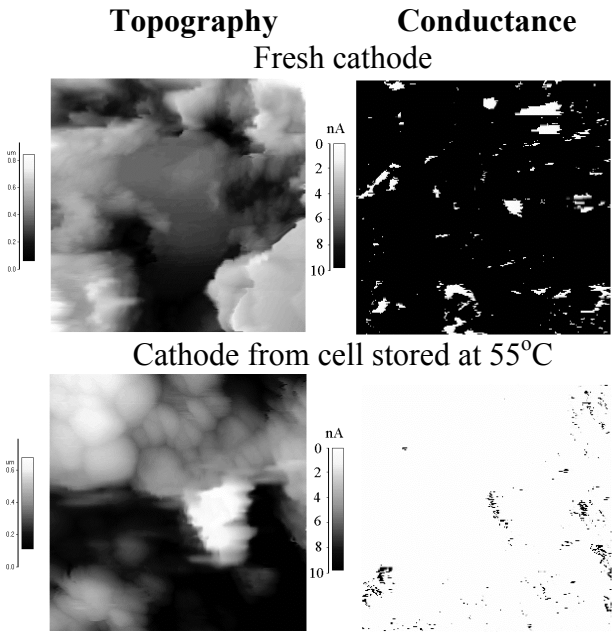

Figure 1. CSAFM images of surface conductance (right-hand panel, black areas are conductive) and topography (left-hand panel) of a 5 x 5 μm region of the cathode surface at 1.0 V tip-sample voltage difference.

The surface conductance image of the cathode from the fresh cell exhibits areas of mostly excellent electronic conductance and only few insulating regions. Highly conductive graphite, acetylene black, and relatively well conducting $LiNi_{0.8}Co_{0.15}Al_{0.05}O_2$ contribute to the observed high tip current. The insulating areas on the cathode surface are most likely associated with the presence of PVDF binder and/or a solid electrolyte interphase (SEI).

The conductance images of cathodes that were stored/cycled at elevated temperatures show a dramatic increase of surface resistance. The conductance image of the cathode stored at 55°C reveals that almost the entire electrode surface became insulating except for a few locations, mainly in the deep crevices and intergranular spaces, which remained conductive.

To gain additional insight into the nature of the observed loss of surface electronic conductance at higher temperatures, we studied the cathode surface with Raman microscopy. The Raman spectra of the fresh cathodes were identical at all locations on the cathode surface; each spectrum is dominated by two groups of bands: a broad maximum centered at ~510 cm^{-1}, characteristic for $LiNi_{0.8}Co_{0.15}Al_{0.05}O_2$ oxide, and two peaks at ~1350 and ~1600 cm^{-1}, which correspond to the D and G bands of elemental carbon, respectively(Fig. 2). In marked contrast to the fresh cathode, the spectral

characteristics the cathode stored or cycled at elevated temperatures varied strongly as a function of location on the cathode surface, suggesting a highly non-uniform cathode surface composition and structure. The broad peak at 500 cm^{-1} split into two peaks at 480 and 550 cm^{-1}, which indicates the presence of at least partially charged $Li_{1-x}Ni_{0.8}Co_{0.15}Al_{0.05}O_2$. Interestingly, the cathode surface SOC varies between and within large individual agglomerates of active material and, at some locations, the spectra correspond to fully charged material, even though the cell was fully discharged at the end of testing and before disassembly.

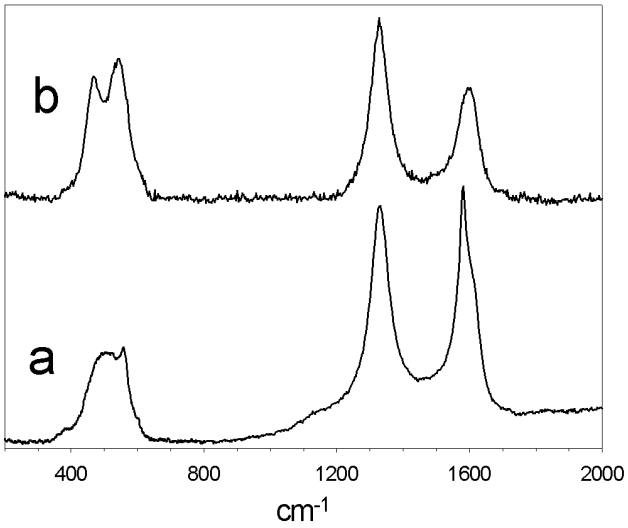

Figure 2. Typical Raman microscope spectra of the fresh composite $LiNi_{0.8}Co_{0.15}Al_{0.05}O_2$ cathode (a), and the cathode from a cell stored at 55°C (b).

A plausible explanation for the observed phenomena could be formation of a very thin SEI layer. A relatively thick layer of Li_2CO_3 and P-, O- and F- containing compounds forms upon storage of $LiNi_{1-y}Co_yO_2$ in $LiPF_6$-containing electrolyte at 80-90°C was found in [5]. However, our Raman and infrared measurements revealed no observable SEI layer on the cathode surface. On the other hand, the presence of charged material at the cathode surface may also indicate that some particles of $LiNi_{0.8}Co_{0.15}Al_{0.05}O_2$ became electrically disconnected from the remaining part of the cathode due to mechanical stress and/or carbon additive retreat. As a matter of fact, Raman microscopy images reveal that cell cycling or storage at elevated temperatures led to significant changes in the $LiNi_{0.8}Co_{0.15}Al_{0.05}O_2$/elemental-carbon local surface concentration ratio [6,7]. However, it should be recognized that the changes in $LiNi_{0.8}Co_{0.015}Al_{0.05}O_2$/carbon surface concentration ratio observed with the Raman microscope may arise from at least two distinct phenomena: (*i*) recession of carbon from the cathode surface, (*ii*) modification of the carbon distribution in the cathode.

By systematically collecting thousands of Raman spectra from a 50 x 80 μm area at 0.9 μm spatial resolution, and integrating the bands of the cathode components of each spectrum, we were able to produce semi-quantitative composition maps of cathode surfaces

Figure 3 shows Raman images of a cathode that showed 16% irreversible capacity loss at the end of testing. Each of the thousands of spectra that constituted the Raman image of the composite cathode was deconvoluted into two components: $LiNi_{0.8}Co_{0.15}Al_{0.05}O_2$ and carbon. The white regions of the image (A) show both charged and discharged oxide whereas the black areas correspond to carbon additive. The Raman image (B) represents the same area of the composite electrode except that the bright areas in this case show only charged oxide. It is clear that some particles of $LiNi_{0.8}Co_{0.15}Al_{0.05}O_2$ became electrically disconnected from the remaining part of the

cathode due to mechanical stress and/or carbon additive retreat. Raman microscopy images of tested cathodes reveal that the cathode surface SOC varies between individual grains of active material and, at some locations, the spectra of fully charged and fully discharged material were recorded within the same large agglomerate (10-20 μm) of $LiNi_{0.8}Co_{0.15}Al_{0.05}O_2$.

A reduction in conductance of portions of the cathode can easily explain the observed loss of cathode capacity *via* isolation of oxide active material. Particle isolation is also in agreement with our observations of carbon retreat or rearrangement in tested cathodes. However, the intrinsic conductivity of the $LiNi_{0.8}Co_{0.15}Al_{0.05}O_2$ (10^{-2}-10^{-3} S cm^{-1}) should be sufficiently high to compensate for a partial conductivity loss within the thin (40 μm) cathode bulk, not to mention individual agglomerates of $LiNi_{0.8}Co_{0.15}Al_{0.05}O_2$.

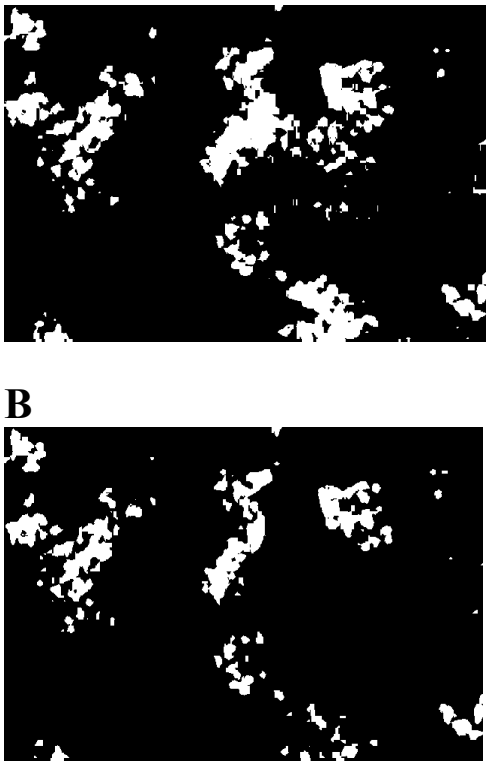

Fig. 3. Raman microscopy 50 x 80 μm surface images of $LiNi_{0.8}Co_{0.15}Al_{0.05}O_2$ composite cathode from a cell surface The bright areas show (A) Charged and discharged active material, (B) Charged active material alone

In order to determine a possible impact of the carbon recession on the performance of the composite cathodes we investigated the intrinsic electronic properties of $LiNi_{0.8}Co_{0.15}Al_{0.05}O_2$ grains. Individual 10-25 μm agglomerates of $LiNi_{0.8}Co_{0.15}Al_{0.05}O_2$ were pressed into a gold foil, and then their local electronic properties were investigated *via* CSAFM. The morphology image and the

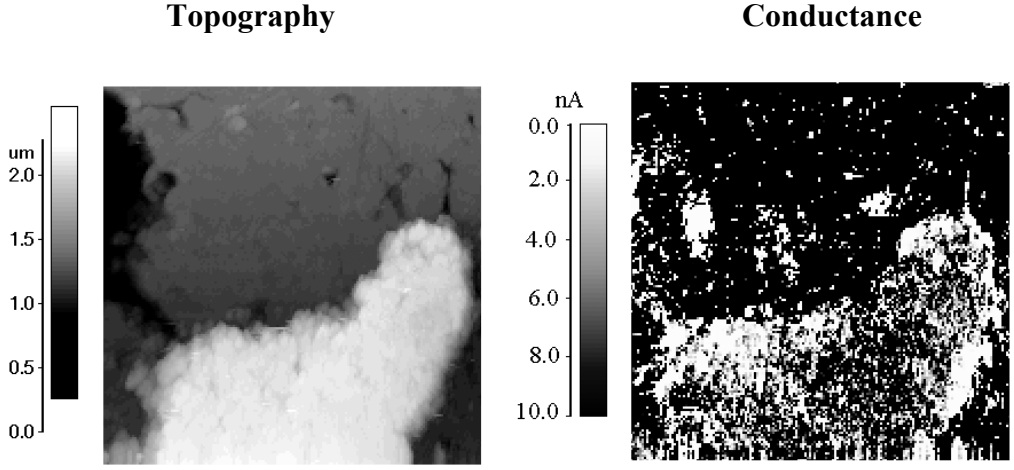

Figure 4. CSAFM 20 x 20 μm images of $Li_{1-x}Ni_{0.8}Co_{0.15}Al_{0.05}O_2$ agglomerates pressed into Au foil. 2.0 V tip-sample voltage difference. (black areas on the conductance image are conductive)

corresponding surface conductance map are shown in Figure 4. Large agglomerates of $LiNi_{0.8}Co_{0.15}Al_{0.05}O_2$ consisted of smaller (from sub-micron to ~1-5 micron) crystallites fused tightly together. The conductance image revealed that the agglomerated crystallites were not uniformly conductive.

Surprisingly, some crystallites displayed good electronic conductivity (as expected) and some exhibited very high resistance. We attribute this non-uniformity in electronic properties to poor inter-crystallite (*i.e.*, inter-granular) electronic contact. This poor contact inhibits electrons from reaching crystallites which are not in direct contact with the Au current collector. The presence of a relatively large amount of carbon additives uniformly distributed in the fresh composite $LiNi_{0.8}Co_{0.15}Al_{0.05}O_2$ cathode provides a conductive path not only between large agglomerates and the Al current collector but also between crystallites within the agglomerates. The excess of carbon neutralizes the inherently poor nascent inter-granular electronic contact because it provides an additional connection path to the current collector through the carbon matrix. Gradually receding (or rearranging) carbon additives can "expose" small crystallites within agglomerates. If these particles were in poor electronic contact with their neighbors then the consequent loss of a direct electronic path through the receding carbon matrix will lead to an increased resistance within the agglomerate and, eventually, total isolation of some particles. Thus, we postulate that the combination of carbon retreat (or rearrangement) and the intrinsic properties of the $LiNi_{0.8}Co_{0.15}Al_{0.05}O_2$ powder is responsible for the observed power and capacity fade of the composite cathodes.

ACKNOWLEGEMENT

This work was supported by the Assistant Secretary for Energy Efficiency and Renewable Energy, Office of FreedomCAR and Vehicle Technologies of the U.S. Department of Energy under Contract No. DE-AC03-76SF00098. The authors gratefully acknowledge the tested cells, help, and advice provided by the ATD Program participants.

REFERENCES

1. "FY 2000 Progress Report for the Advanced Technology Development Program," U.S. Department of Energy, Office of Advanced Automotive Technologies, Washington, D.C. (December 2000).
2. A. X. Zhang, P. N. Ross, Jr., R. Kostecki, F. Kong, S. Sloop, J. B. Kerr, K. Striebel, E. Cairns, and F. McLarnon, *J. Electrochem. Soc.* **148**, A463 (2001).
3. R. Kostecki and F. McLarnon, *Electrochem. Solid State Lett.,* **5***,* A164 (2002).
4. D. P. Abraham, R. D. Twesten, M. Balasubramanian, J. Kropf, D. Fischer, J. McBreen, I. Petrov, K. Amine, *J. Electrochem. Soc.***, 150**, A1450 (2003).
5. D. Ostrowskii, F. Ronci, B. Scrosati, and P. Jacobsson, J. Power Sources, **94**, 183 (2001).
6. R. Kostecki and F. McLarnon, submitted to *Electrochem. Solid State Lett.,*
7. K.A. Striebel, J. Shim, E.J. Cairns, R. Kostecki, Y.-J. Lee, J. Reimer, T.J. Richardson, P.N. Ross, X. Song, G. V. Zhuang, submitted to *J.Electrochem. Soc.,*

Key words: : Li-ion battery, cathode, carbon retreat, conductivity, micro-Raman, AFM